

Simulation and experimental validation of phase change material and water used as heat storage medium in window applications

Benjamin Durakovic^{1*}, Muris Torlak²

¹International University of Sarajevo, 71210 Ilidža, Bosnia

²University of Sarajevo, Vilsonovo Setaliste 9, 71000 Sarajevo, Bosnia

Received 19 May 2016,
Revised 26 Oct 2016,
Accepted 31 Oct 2016

Keywords

- ✓ Phase change material;
- ✓ Energy storage;
- ✓ Simulation;
- ✓ Interior glass surface temperature variation

bdurakovic@ius.edu.ba,
Phone: +387 33957 229

Abstract

Performances of two different materials (*water and phase change material*) were studied as heat storage medium in passive design of buildings. An experimental and numerical simulation method was applied. The experimental study was conducted in the laboratory environment on double glazed window sample. Numerical simulation model was formulated to simulate the transient heat transfer through the window system. The results show that the PCM filled window can be protected from rapid overheating due to latent heat of the phase change material. Numerical model showed good matching with experiment; therefore, the model can be used for the window system performance evaluation as energy storage unit under different configurations.

1. Introduction

Energy consumption in building sector through heating and cooling is considerable and takes up to 40% of global energy consumption [1]. Reducing building energy demand is challenging but achievable, for example through better insulation of building envelope using new materials and approaches. Emerging technologies based on application of phase change materials (PCM) in building envelope for energy storage [2] can enhance the thermal performances of buildings [3] but PCM degradation may happen due to thermal cycling [4]. These materials use latent heat of fusion to store relatively large amounts of energy for later usage, at narrow temperature ranges [5]. The PCMs are applied directly into the building structure [6] such as plaster [7], concrete [8], brick [9] and building components such as windows.

Some experimental and numerical studies of thermal performances of a PCM window system were conducted. Authors were concerned to simulate storage process in various types of PCM applications in windows such as interior shading devices [10,11], exterior shading devices [12,13], and window integrated storage system [14].

Integrated shading system

Researchers applied PCM and water as heat storage materials in the glazing cavity with the aim of lowering glazing system temperature and preventing the window from overheating. The concept solutions are dependant of micro controller and circulating pump for moving of liquid PCM or water from the cavity [15].

In case of the PCM-filled window, load shifting effects and thermal performances of the window system have better performances in hot climate regions [16] [17] while in cold climate regions low potential of window system is presented due to inability of completing phase transition process [18]. Thermal performances of the PCM window system can be increased by enhancing thermo physical parameters of new PCMs such as latent heat and phase transition temperature in the range of 25–31°C [19] [20]. The PCM filled window system offers acceptable translucence in solid phase [21] and transparency in the liquid phase [22] [23].

In case of water-filled window, the glazing cavity was used as water heater for remote sanitary water tank. Thermal characteristics of water-flow double-glazed window concept and its annual performances were studied [24]. Researchers claim that the concept has higher potential of removing the heat by lowering the glazing temperature than the traditional ventilation [25] [26].

The aim of this study is to introduce and validate numerical model that can be used in studying of thermal effects of PCM and water applied in integrated glazing systems exposed to the environment with convective

heat transfer and its effect in reducing building cooling demand. The needs for this study are reflected in its contribution to the development of environmentally responsive building components [27] based on the energy storage, which will reduce building energy demand and foster passive design strategies.

The previous studies were focused on possibilities of application of the PCM in interior, exterior and integrated glazing systems and building structure. Also several studies have been concerned to the application of the water in integrated glazing systems as heat storage medium. In terms of integrated glazing systems in the previous studies, additional devices such a pump and piping system were used to foster water or liquid PCM circulation, which are not suitable in passive design strategies. In this work, another approach suitable for passive design is used to investigate effects of the storage materials used in the system on the interior glass surface temperature. A double glazed window system model free of circulating pump was introduced and analyzed using experimental and numerical methods.

2. Research Methods

Experimental Method

With the aim of validating numerical result, experiments were conducted in the laboratory environment including convection and conduction heat transfer modes. The schematic diagram of the experimental setup used for sample analysis of the melting and solidification characteristics during heating and cooling processes are shown in Figure 1.

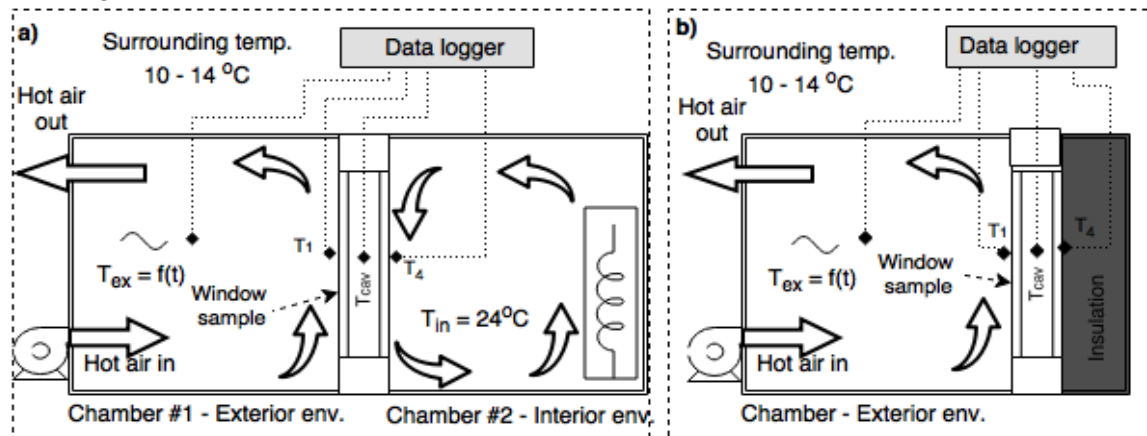


Figure 1: Experimental setup: (a) convective boundary; (b) adiabatic boundary

Referring to Figure 1, convective heat transfer experiment was conducted in the lab environment using two test chambers. Chamber #1 represents exterior environment while Chamber #2 represents interior environment. Chambers were made out of 25mm plywood with dimension of each chamber $W \times L \times H = 120 \times 75 \times 75$ cm, while 5mm cork sheet was installed on the interior side of the chamber.

Diamond signs in Figure 1 represent positions of temperature sensors. The temperature was recorded every four seconds at exterior glass surface; interior glass surface; and between glazings in the cavity. Temperature control in each chamber (T_{ex} and T_{in}) over a day cycle is achieved by using controller. Since Chamber #2 represents interior environment, T_{in} was kept at 24°C over the cycle, which represents interior design temperature for summer season [28].

To describe desired temperature variation inside chamber #1 that corresponds to temperature variation of an average summer day cycle, a control function is used (see Eq.(1)). The temperature variation is maintained by a heater. The heater takes fresh air from the outside of the chamber, heat it and blow it to the chamber at the bottom, while exhausted air leaves the chamber at the top.

$$T_{ex}(t) = \frac{1}{2}(T_{ex,max} - T_{ex,min}) \cdot \sin\left(\frac{t}{\omega} \cdot 2\pi\right) + \frac{1}{2}(T_{ex,max} + T_{ex,min}) \quad (1)$$

where, $T_{ex,max}$ is maximum daily temperature of Chamber #1 in $^{\circ}\text{C}$ (at noon reaches daily values of 35°C), $T_{ex,min}$ is minimum daily temperature of Chamber #1 (falls to the value of 17°C), ω is the cycle length in seconds. The temperature of the room in which chambers were placed over day-night cycle was in the range $10 - 14^{\circ}\text{C}$. This ensures the cooling of Chamber #1 at $T_{ex,min}$ temperature.

Computational Method

Heat transfer and the flow of the PCM liquid-phase are governed by the conservation equations of continuum mechanics, describing the balance of mass, momentum and energy [29]:

$$\frac{\partial}{\partial t} \int_V \rho dV + \oint_S \rho \vec{v} d\vec{S} = 0 \quad (2)$$

$$\frac{\partial}{\partial t} \int_V \rho \vec{v} dV + \oint_S \rho \vec{v} \otimes \vec{v} d\vec{S} = - \oint_S p d\vec{S} + \oint_S \boldsymbol{\sigma}_{ns} d\vec{S} \quad (3)$$

$$\frac{\partial}{\partial t} \int_V \rho h dV + \oint_S \rho h \vec{v} d\vec{S} = \oint_S \lambda \text{grad } T d\vec{S} + \int_V q dV \quad (4)$$

The mass and momentum equation (2) and (3) are solved in liquid-phase regions only, while the energy equation is solved both in the liquid and the solid phase of PCM.

In the equations given above, V is the control volume bounded by the closed control surface \vec{S} , t is the time, ρ is the density of the material, \vec{v} is the velocity vector of the liquid phase of PCM, p is the pressure of the liquid phase of PCM, $\boldsymbol{\sigma}_{ns}$ is the shear stress tensor, h is the specific enthalpy, T is the temperature, λ is the thermal conductivity, q is the volume-based heat source or sink.

Non-spherical part of the shear stress tensor $\boldsymbol{\sigma}_{ns}$ is related to the shear rate $\dot{\boldsymbol{\epsilon}}$ using linear relation for Newtonian, incompressible, viscous fluids: $\boldsymbol{\sigma}_{ns} = 2\mu \dot{\boldsymbol{\epsilon}}$, where μ is the dynamic viscosity of the liquid phase.

The specific enthalpy arising in Eq. (4) is defined as:

$$h = \int_{T_0}^T c_p dT + (1 - f_s) H_L \quad (5)$$

where c_p is the specific heat capacity of the PCM, H_L is its latent heat of phase change, and f_s is the volume fraction of the solid phase. In this work, the volume fraction variation with temperature is adopted to be linear from 1 to 0 between solidus and liquidus state. The material properties, density, specific heat capacity and thermal conductivity, are assumed to have constant, but different values depending on the phase of PCM.

Substituting h in Eq. (4) by Eq. (5), the latent heat contribution is added to the volume-based heat source term q . The surface-based heat source q_S may include the contribution of the solar radiation in cases where this is taken into account. The computations were done using commercial CFD software STAR-CCM+. The equation discretization allows the use of unstructured computational grids consisting of arbitrary polyhedral, contiguous, non-overlapping cells in the domain of interest, and follows the finite-volume approach by Demirdžić et. al. and Muzaferija et al., which is reported in STAR-CCM+ User Guide [30]. In this work, however, Cartesian grids are used due to simple geometry of the problem under consideration. The conservation equations is applied to the solution domain as a whole, as well as to each cell in the grid. Assembling discretized conservation equations for each cell, systems of equations are built for velocity and pressure (in the liquid phase only) and temperature (in both phases) at the cell centers, and are solved sequentially in turn [29]. The method results in discretization error of the 2nd-order, both in space and time.

Computational model

Figure 2 shows the computational model considered in this paper. The model loses or gains heat from the interior and exterior ambient by convection and conduction.

The glass thickness is L_g is 4 mm, while the cavity between the glass plates L_{cav} was 12 mm. The weather conditions are selected per ASHRAE 2009 handbook, with typical values holding on September 22 for Sarajevo, Bosnia [28]. Nominal heat transfer coefficient values at the exterior and interior surfaces are $\alpha_{ex} = 25$ W/m²K and $\alpha_{in} = 8$ W/m²K respectively [28]. Depending of the case, interior glass surface was considered as convective or adiabatic. Indoor air temperature was kept constant at 24 °C while the interior glass surface temperature (T_4) was calculated.

The side boundaries are regarded as adiabatic, implying herewith a 1D analysis in horizontal direction. The number of cells across the cavity was 42 cells. The adopted time step size is reduced down to 4 s, which is found to be sufficiently fine with respect to the characteristic period of temporal variations. The computational models are exposed to heat variation originating from exterior air temperature over a 3 x 24 hour cycle [31].

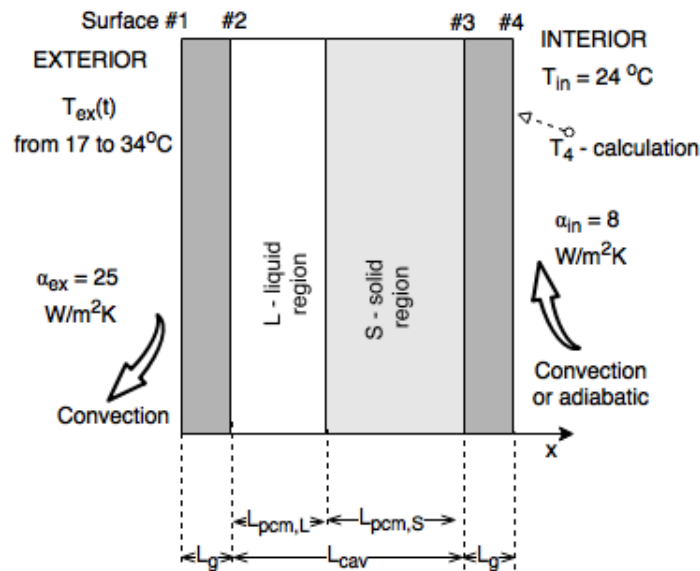


Figure 2: Computational model

The PCM applied in simulations and experiments is commercially available paraffin RT27 from Rubitherm GmbH. The physical properties of the PCM used in the simulation are given in Table 1, based on the manufacturer's technical datasheet [32], while the properties of water and air are taken from the standard literature [33].

Table 1: Physical properties of the PCM Rubitherm RT 27

Name	Value
Density, solid phase	880 kg/m ³
Density, liquid phase	760 kg/m ³
Dynamic viscosity, liquid phase	0.02 Pa s
Specific heat (both phases)	2000 J/kgK
Thermal conductivity (both phases)	0.2 W/mK
Latent heat	189 kJ/kg
Solidus temperature	24.5 °C
Liquidus temperature	26.5 °C

In developing the PCM computational model some assumptions have been used. Referring to Figure 2, the convection process in the cavity during melting is neglected but in the reality may be presented; the melting process is ongoing layer by layer parallel to the exterior glass surface; the heat transfer through the glass surface is uniform.

3. Results and Discussion

Convection and Conduction Results

Results are shown for two types of the boundary conditions on interior glass surface, convective and adiabatic. Convective boundary condition represents real case temperature fluctuation on the interior glass surface. Adiabatic case was analyzed with the aim of assessment of interior glass surface temperature fluctuation when the impact of convection is eliminated. Both cases are investigated experimentally and numerically over 72 hour period and compared.

Experimental results are used to validate computational model results. Series of experiments were conducted in the lab for both configurations (convective and adiabatic boundaries) and for all three materials (air, water, PCM). The following figures (Figure 3 & Figure 4) show the results obtained by experimental lab tests for different configurations. Temperatures were recorded on the exterior glass surface (T_1), in the cavity (T_{cav}) and on interior glass surface (T_4) for each material.

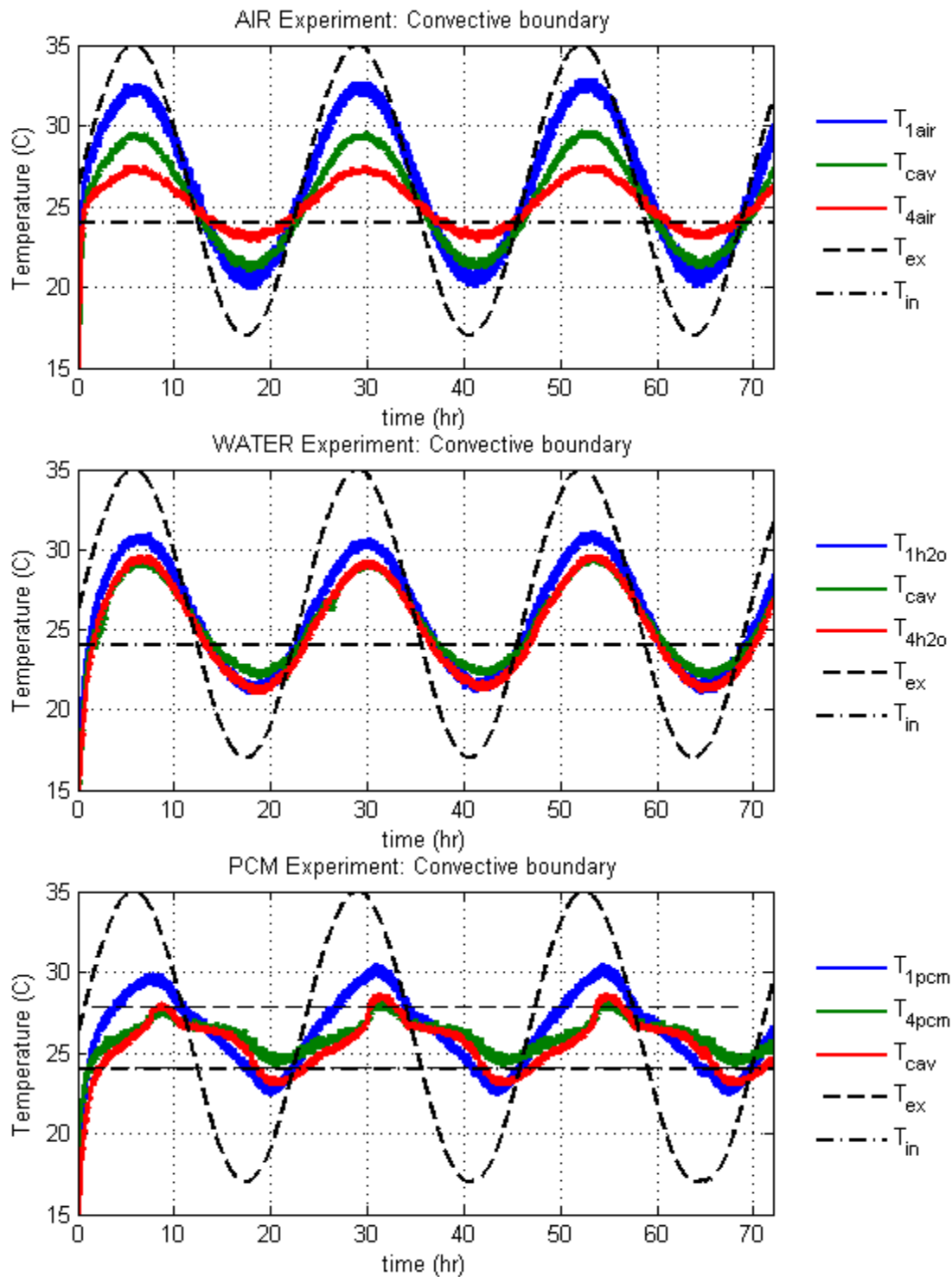


Figure 3: Convective boundary for samples filled with air, water and PCM (T_{ex} - exterior air temp.; T_{in} - interior air temp.)

Convective component of transient heat transfer is tested on samples of water, air and PCM material. Depending on the material and experiment type, the different temperature distributions were observed through the glazing system.

Air temperature difference between interior and exterior glass surface is about 5°C at peak temperature. The high temperature difference is a result of low air conductivity, which is good as thermal insulator. Therefore high temperature oscillations on the exterior glass surface is observed (about 11°C), while the interior glass surface temperature oscillations is about 5°C . As the air has relatively low specific heat capacity therefore the heat accumulation in the air between the glazings is inconsiderable. Once the exterior air temperature falls below room temperature, this change was shortly reflected on the interior glass surface in an hour.

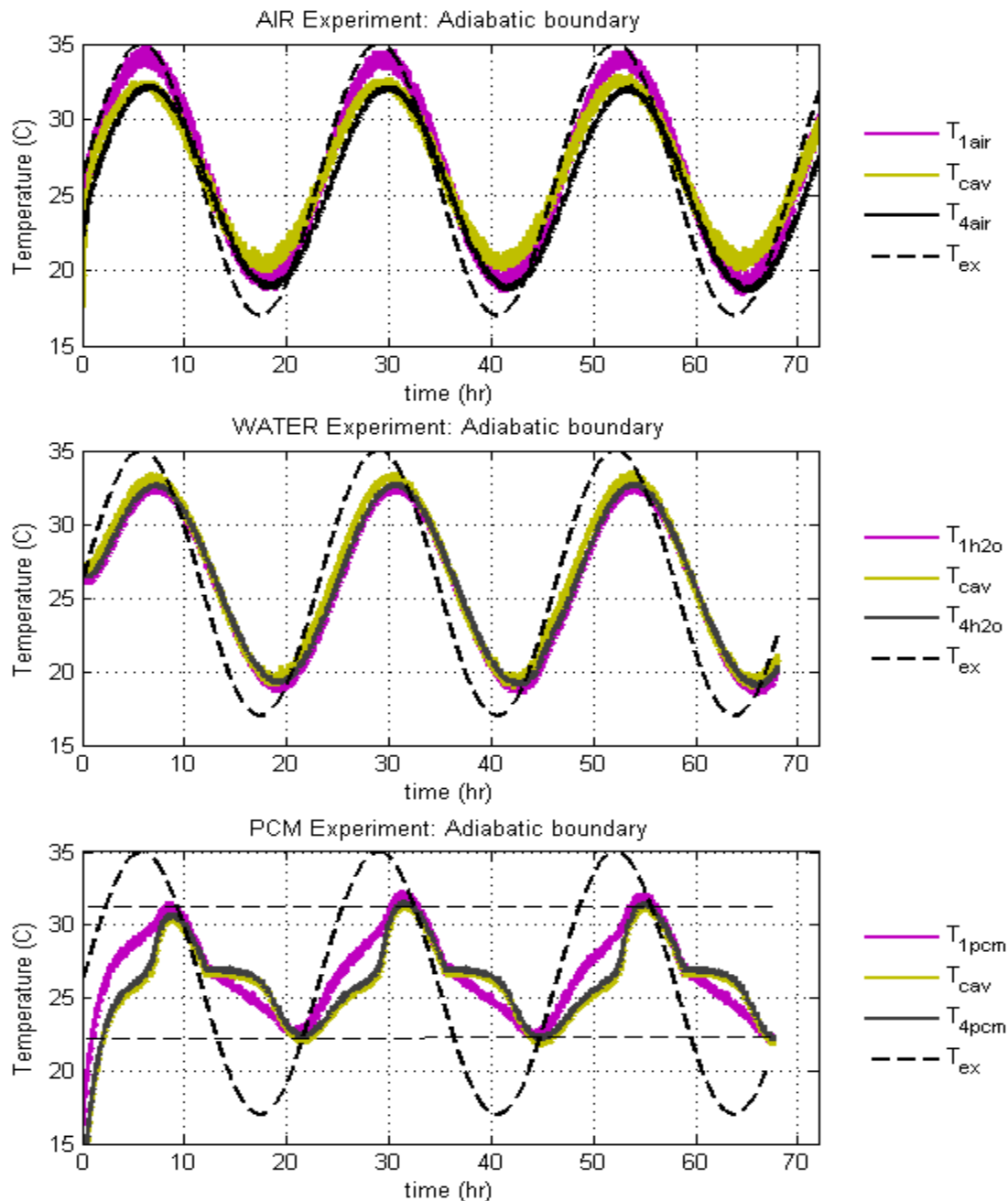


Figure 4: Adiabatic boundary for samples filled with air, water and PCM

In case of water filled glazing, the peak temperature difference between exterior and interior glass surface is about 2 °C, which is the result of relatively higher thermal conductivity of the water. Compared to the air filled glazing, it is observed that variation of exterior glass surface temperature is about 2°C lower but interior surface temperature is for about 4°C higher. Relatively higher specific heat capacity of the water enables absorbing the heat and causing the reduction of the exterior glazing temperature for about two degrees. Increased variation of interior glazing temperature is caused by relatively higher thermal conductivity of the water. Thus, the interior glass surface temperature change is more sensitive to the exterior temperature change, and therefore the water is considered as unfavorable material for energy storage between the glazings.

It was observed that the PCM filled glazing system has much lower temperature fluctuations on the exterior and interior glass surfaces. The heat is absorbed by the PCM in the form of latent heat by maintaining the interior glass surface temperature lower. Temperature flattening effect over the melting and solidification period is observed by providing the longest period of almost uniform temperature on the interior glass surface. Therefore, the window is not sensitive to sudden external temperature changes because the accumulated latent heat in the PCM is able to maintain interior glass surface temperature for about 4 hours after the exterior air temperature falls below room temperature.

The previous results were verified by applying adiabatic boundary condition on the interior glazing surface with the aim of eliminating the effect of interior convection. The result is shown in Figure 4. Considerably higher peak temperatures at all planes with all materials were observed. The reason is that the heat release on the interior side is not allowed. Thus, reduction of the temperature in the interior surface of the air filled cavity is considerably limited.

The PCM shows, however, temperature curve flattening effect, which results for a certain period of time (between 13h and 19h), as lower values of temperature on the interior surface than with the other two materials. The same phenomenon and temperature trends were observed; therefore the same conclusions can be drawn for adiabatic boundary condition as it was mentioned earlier for the convective boundary condition.

Experimental vs. Simulation Results Discussion

Simulation results are compared with experimental for each material in the cavity considering both boundary conditions on the interior glass surface. Convective boundary case with interior air temperature of $T_{in} = 24^{\circ}\text{C}$, and adiabatic boundary on the interior glass surface were analyzed. With the aim of numerical model validation, the results of numerical simulation are compared to the experimental results and shown in

Figure 5.

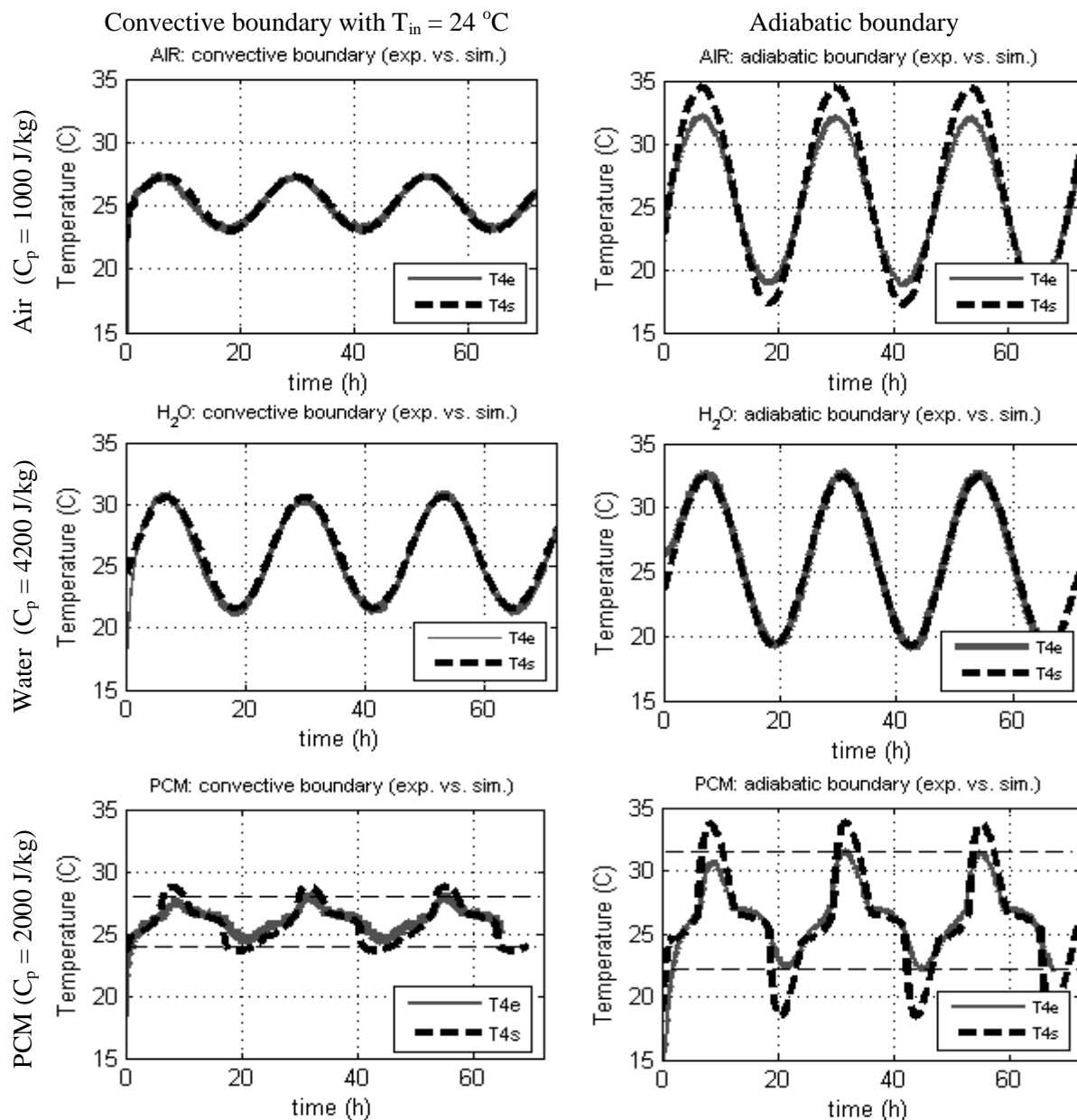


Figure 5: Interior glass surface temperatures - experimental vs. simulation results: T_{4e} - experimental; T_{4s} - simulation (validated on 12 mm cavity)

Since numerical model considers ideal one dimensional heat transfer, which is not case in the reality, thus model error is more associated with the adiabatic boundary condition case compared to the convective. It can be explained with the amount of heat accumulated in the material, which depends of the material heat capacity, or numerical error. Specific heat capacity value provided by manufacturer of the PCM and used in the computation might be incorrect, it seems that in solid and liquid in is higher than in the reality. Additional reason of the error can be explained by impossibility of achieving the adiabatic boundary condition within lab environment while it is possible by computational model. Although, adiabatic boundary condition in the experimental model eliminates influence of convection on the interior side of the glass, however the ideal adiabatic condition is not achieved. Some heat exchange through the insulation and surfaces in contact with the surrounding wall is taking place over the time. Since the computational model does not take these heat exchanges into account, some discrepancies between the experimental results and the results obtained by the simulation are observed. Simulation results show more heat is remained in the material (PCM, air, water) by increasing the temperature of the glazing system proportional to material heat capacities.

In the case of convective boundary conditions there is a certain heat transfer ongoing through the interior glazing causing very slow cooling of the PCM. In the adiabatic case this heat is not presented and therefore the PCM heats and cools rapidly which is expressed through the excessive temperature variation on the interior glass surface.

In the following figures (Figure 6 & Figure 7), three cycles of T_4 temperatures on the interior glass surface are compared for all three materials in the cavity. Figure 6 shows the experimental results obtained in the laboratory for the convective boundary condition while the Figure 7 shows the computational results for the same conditions. In both cases each material has the same temperature trend for each cycle, so the same conclusion can be drawn. PCM temperature flattening provides the longest period of indoor temperature control over melting and solidification process.

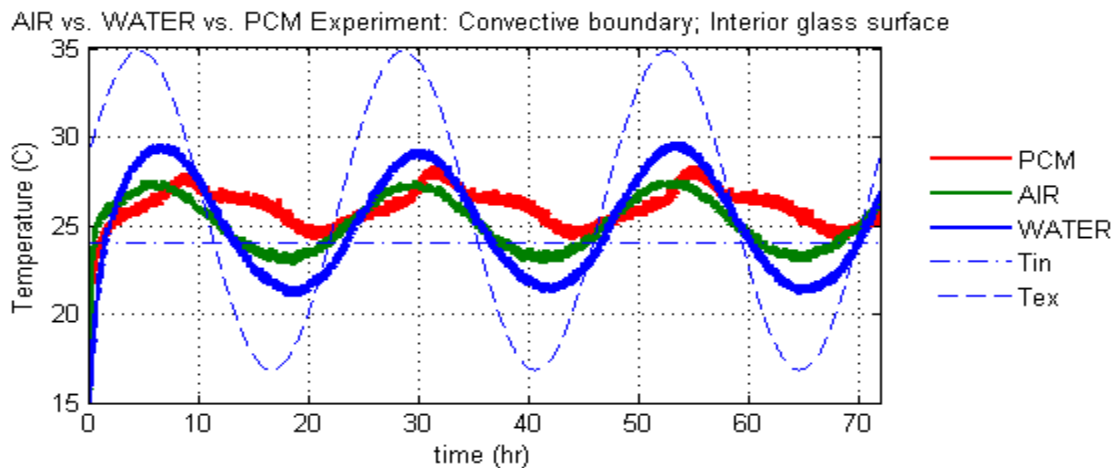


Figure 6: Interior glass surface temperature variation for the air, PCM and water (experimental results)

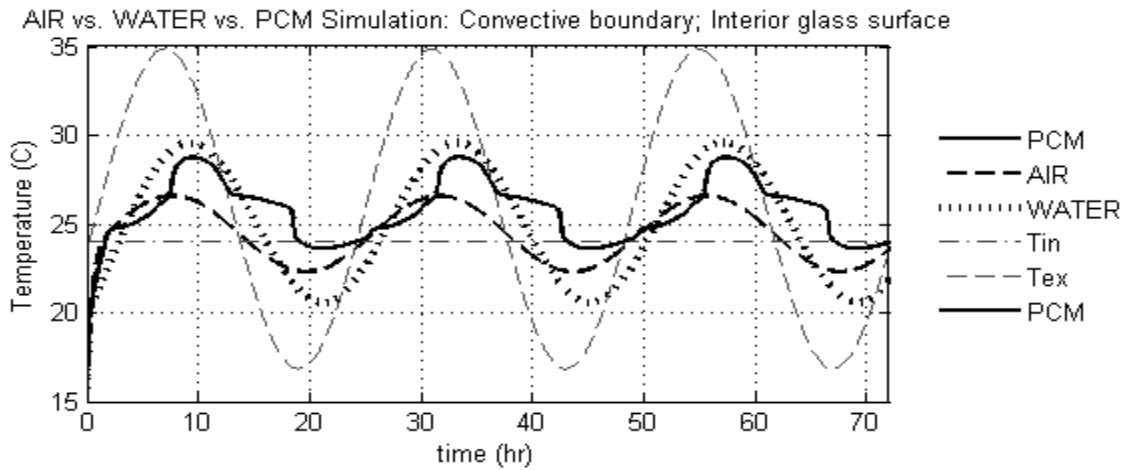


Figure 7: Interior glass surface temperature variation for the air, PCM and water (computational results)

Referring to Figure 6 & Figure 7, it is shown that different materials have different impact on the indoor temperature. Specific heat capacity of 4.2 kJ/kgK qualifies the water as material with very good thermal mass for physical heat storage. Due to high heat conductivity, T_4 temperature associated with the water is the highest and the heat gain to the interior is the highest per unit of time. These features make the water as most unfavorable material in the cavity. Conductivity of 0.02 W/mK qualifies the air as very good insulator and resulting with a moderate variation of T_4 temperature. The heat capacity of 1 kJ/kgK qualifies the air as bad thermal mass material to absorb and retain the heat for later usage. As that, the air follows temperature change which has the impact to the heating and cooling load.

Utilizing the effect of stored latent heat the PCM provides a small T_4 temperature variation reflected through the flattening temperature curve. When the exterior temperature is increased above the room temperature the PCM absorbs the heat during the melting process allowing the temperature to rise for 2 degrees over the melting cycle. Temperature increase of melted PCM (Figure 6) goes one degree higher than the maximum air temperature but only for short period of two hours. As result of the releasing the heat to the room during the solidification process, another three hours of the temperature curve flattening are presented by shifting and reducing the load of the air-conditioning (A/C) system. The results of this study are also compared with the previous studies and discussed in Table 2 and Table 3.

Table 2: Previous study results and comparison for PCM

Author / Reference	Temperature flattening period (h)	Transition / peak temperature (°C)	Comment
Zhong et al. [17] and [19]	6	31/32	Transition temp. is 31 °C, thus requires cooling during the transition period of 6h. Partial cooling outside is enabled.
Ismail et al. [34]	5	24/30	Shorter transition period of 5h. Partial cooling outside is enabled.
Li et al. [23] and [20]	10	28/32	10 h of transition period around 28 °C. Partial cooling outside is enabled.
This study	15	26/28	Provides transition period of 15h at surf. temp. of 26°C., tested on 12mm cavity. Increased cavity thickness extends the period as stated in [35]

Table 3: Previous study results and comparison for water

Reference	temperature reduction (°C)	Comment
[24] [25] [26]	3	Reduced temperature between interior and exterior glass surfaces for 3°C with water circulation.

Comparing performances of water and PCM as heat energy storage medium in glazing application it is obvious that water had higher temperature fluctuation and as overall the PCM may provide the most benefits for the A/C load by delaying heating or cooling due to its latent heat.

Conclusion

It was shown good matching between computational and experimental results for both cases convective and adiabatic boundary conditions at interior glass surface. Since convective and adiabatic case results have the same trends therefore, the convective case as more realistic behavior of the glazing system and can be used in the computational models as predictor of temperature variation.

Applying PCM in the glazing systems and taking advantage of its latent heat can be beneficial in reducing indoor temperature fluctuation. Latent heat of melting and solidification has flattening effect on interior glass surface temperature histories by reducing peak temperatures. Compared to the water, the peak temperature is reduced for 2 degrees by protecting the window system from rapid overheating. Thus the PCM may be considered as better performance material for energy storage and balancing.

References

1. Pérez-Lombard L., Ortiz J., Pout C. A., *En. and Build.* 40 (2008) 394.
2. Khyad A., Samrani H., Bargach M.N., *J. of Mat. and Env. Sci.* 4 (2016) 1184.
3. Silva T., Vicente R., Rodrigues F., 53 (2016) 515.
4. Goia, F. & Boccaleri, E., *En. and Build.* 119 (2016) 41.
5. Benomar W., Zennouhi H., Arid A., Rhafiki T.E., Msaad A.A., Kousksou T., *J. of Mat. and Env. Sci.* 6 (2015) 3416.
6. Soares, N., Costa, J. J., Gaspar, A. R. & Santos, P., *En. and Build.* 59 (2013) 82.
7. Liu H., Awbi H., *Build. and Env.* 44 (2009) 1788.
8. Cabeza L., Castello'n C., Nogus M., Medrano M., Leppers R., Zubillaga O., *En. and Build.* 39 (2007) 13.
9. Castell A., Martorell I., Medrano M., Prez G., Cabeza L., *En. and Build.* 42 (2010) 534.
10. Weinlaeder H., Koerner W., Heidenfelder M., *En. and Build.* 43 (2011) 2468.
11. Silva, T., Vicente, R., Rodriguea, F., Samagaio, A. & Cardoso, C., *En. and Build.* 88 (2015) 110.
12. Alawadhi E.M., *En. and Build.* 47 (2012) 421.
13. Soares N., Samagaio A., Vicente R., Costa J., *Proceedings of WREC, Linköping, Sweden*, (2011).
14. Merker O., Hepp F., Beck J., Fricke J., *Proc. of the World Renewable Energy Congress VII*, (2002).
15. Ismail K.A.R., Henriquez J.R., *Applied Thermal Engineering*, 21 (2001) 1909.
16. Zhong K., Li S., Sun G., Zheng J., Zhang X., *6th Int. Build. Phy. Conf., IBPC2015*, (2015).
17. Li S., Zhong K., Zhou Y., Zhang X., *En. and Build.* 85 (2014) 483.
18. Grynning S., Goia F., Time B., *En. Proc.* 78 (2015) 85.
19. Zhong K., Li S., Sun G., Li S., Zhang X., *En. and Build.* 106 (2015) 87.
20. Li D., Li Z., Zheng Y., Liu C., Hussein A.K., Liu X., *Solar Energy*. 133 (2016) 207.
21. Goia F., Zinzi M., Carnielo E., Serrad V., *En. and Build.* 87 (2015) 302.
22. Gowreesunker B.L., Stankovic S.B., Tassou S.A., Kyriacou P.A., *En. and Build.* 61 (2013) 239.
23. Li D. et al., *En. and Build.* 119 (2016) 143.
24. Li C. & Chow T.-t., *Procedia Env. Sci.* 11 (2011) 1039.
25. Chow T.T., Li C., Lin Z., *Int. J. of Ther. Sci.* 50 (2011) 140.
26. Chow T.T., Li C., Lin Z., *Build. and Env.* 46 (2011) 955.
27. IEA International Energy Agency, "Annex 44 integrating environmentally responsive elements in buildings," IEA International Energy Agency, Energy Conservation in Buildings & Community Systems, 2011. [Online]. Available: <http://www.ecbcs.org/annexes/annex44.htm>. [Accessed 15 August 2016].
28. *ASHRAE Handbook of Fundamentals*. (2009).
29. Ferziger, J. H. & Peric, M., *Computational Methods for Fluid Dynamics* (2002).
30. CD-Adapco. *Uer Guide - STAR-CCM+ Version 8.06*: 2013.

31. Torlak M., Delalić N., Duraković B., Gavranović H. *Energy Technologies Conference - ENTECH '14*, (2014).
32. Rubitherm. ORGANIC PCM – RT. <http://www.rubitherm.eu/> November 2015.
33. VDI. *VDI Heat Atlas. Dusseldorf: Springer Berlin Heidelberg*; (2010).
34. Ismail K. A. R., Salinas C. T. & Henriquez, J. R., *Energy and Build.* 40 (2008) 710.
35. Durakovic B. and Torlak M., *Int. J. of Low-Carbon Tech.*, 2016, In Press.

(2017) ; <http://www.jmaterenvironsci.com>